Transactions on Modelling and Simulation vol 18, © 1997 WIT Press, www.witpress.com, ISSN 1743-355X

Reconstruction of traction from subsurface strain data in three-dimensional elasticity using BEM

Fan Zhang, Alain J. Kassab, and David W. Nicholson
Institute for Computational Engineering
Department of Mechanical, Materials, and Aerospace Engineering
University of Central Florida, Orlando, FL 32816-2450, USA
Email: kassab@pegasus.cc.ucf.edu

Abstract

An inverse algorithm is developed in this paper to reconstruct boundary tractions from internal strains in three-dimensional elasticity using the boundary element method. The numerical instability problem associated with the solution of the inverse elasticity problem is overcome by employing a polynomial approximation of the unknown traction. Introduction of the polynomial approximation has the combined effect of enforcing smoothing conditions and reducing the number of unknowns. Further, global equilibrium conditions are also enforced to reduce the error in the computed tractions. As a result, stable solutions are obtained even for input strains with significant amount of random errors. Numerical examples are given to validate the proposed inverse algorithm.

1 Introduction

This paper addresses the three-dimensional traction reconstruction problem in which tractions are incompletely specified and need to be reconstructed using strain data provided by experimental measurements at a number of points inside the solid body. In practice, subsurface strains can be measured using fiber optic strain sensors[1]. However, in this study, input strains are simulated by numerically calculated strains. Measurement errors in experiments are considered by introducing random errors to the numerically calculated strains. The solution of the inverse traction reconstruction problem finds application in

evaluation of residual stress and contact stress from experimental data[2-5]. Previous research of the boundary traction reconstruction problem has been concentrated on two-dimensional cases[2-9]. This study shows that the numerical instability problem becomes more severe in three dimensions. Consequently, solution schemes for two dimensional problems such as the one proposed previously by the authors[2] cannot be directly extended to the three-dimensional case. This difficulty is overcome by employing a global polynomial traction approximation and by introducing additional constraints in the form of overall equilibrium conditions. In contrast to the regularization method[6] and SVD[8], these constraints have clear physical meaning. Numerical examples reveal good tolerance to input error for the algorithm.

2 Inverse traction reconstruction and BEM solution algorithm

The inverse problem considered in this paper is defined through an example illustrated in Fig. 1. The boundary Γ of a solid body Ω consists of three parts with prescribed displacements u_1 on Γ_1, prescribed tractions t_2 on Γ_2, and both displacements u_3 and tractions t_3 as unknowns on Γ_3. The unknown traction t_3 is defined as the primary unknown, and all other unknown boundary conditions are secondary unknowns. Strains are measured at several internal points close to Γ_3. The objective is to determine t_3 from measured strains. The governing field equations are the same as in a forward problem.

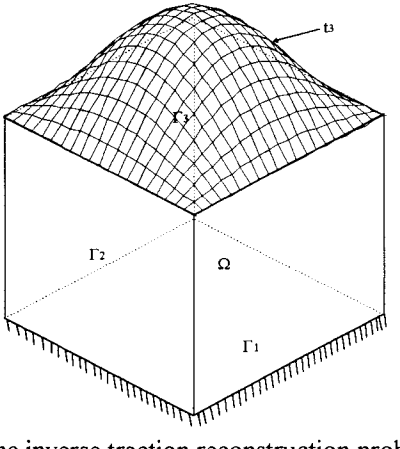

Figure 1. Definition of the inverse traction reconstruction problem.

The first step of the solution is to express internal strains in terms of primary unknown t_3 and other known quantities. In linear elasticity, displacement and stresses are completely determined by boundary conditions and body forces. Thus, internal strains can be expressed as:

$$\epsilon(\xi) = \mathrm{L}(u_1(\underline{X}),\, t_1(\underline{X}),\, u_2(\underline{X}),\, t_2(\underline{X}), u_3(\underline{X}),\, t_3(\underline{X}), b(X)) \qquad (1)$$

where L denotes a linear operator, ξ denotes an internal strain measuring point, $\underline{X}$ denotes any boundary point, and X denotes any point in the domain. If secondary unknowns t_1, u_2 and u_3 are expressed as a linear function of primary unknown t_3 and prescribed boundary conditions, then Eq. (1) can be written as:

$$\epsilon(\xi) = \mathrm{L}'(u_1(\underline{X}),\, t_2(\underline{X}),\, t_3(\underline{X}),\, b(X)) \tag{2}$$

where L' is a linear operator. A discretized form of the above relation is given in the following matrix form:

$$\{\epsilon\} = [C]\{t_3\} + \{b\} + \{d\} \tag{3}$$

Here, vector $\{\epsilon\}$ is the computed strain vector and $[C]$ is the sensitivity matrix. Vector $\{b\}$ accounts for internal strains due to prescribed displacements u_1 on Γ_1 and prescribed tractions t_2 on Γ_2. Vector $\{d\}$ accounts for internal strains due to body forces. Once matrix $[C]$ and vectors $\{b\}$ and $\{d\}$ are formulated, $\{t_3\}$ can be determined by matching computed strains to measured strains. In the following, Eq.(3) is derived using a BEM approach.

Following standard BEM discretization of the boundary and interpolation of the displacements and tractions within each element, the boundary integral equations for displacements and strains can be written as[10]:

$$u_i(\xi) = \sum_{k=0}^{\mathrm{n}K} G_{ik}\, t_k + \sum_{k=0}^{\mathrm{n}K} H_{ik}\, u_k + f_i \tag{4}$$

$$\epsilon_{ij}(\xi) = \sum_{k=0}^{\mathrm{n}K} E_{ijk}\, t_k - \sum_{k=0}^{\mathrm{n}K} F_{ijk}\, u_k + g_{ij} \tag{5}$$

where K is the number of boundary nodes and n is the number of dimensions. Here, u is the displacement, t is the traction, ϵ is the strain, and f and g are body force terms. Influence coefficients $G_{i,j}$, $H_{i,j}$, $E_{i,j}$, and $\mathrm{F}_{i,j}$ are computed via quadrature[10]. Collocating the first equations at all K boundary nodes and the second equation at all M internal measuring points, Eqs. (4-5) become:

$$[H]\{u\} = [G]\{t\} + \{f\} \tag{6}$$

$$\{\epsilon\} = [E]\{t\} - [F]\{u\} + \{g\} \tag{7}$$

Matrices $[H]$ and $[G]$ have dimension $\mathrm{n}K \times \mathrm{n}K$, and matrices $[E]$ and $[F]$ have dimension $M \times \mathrm{n}K$. Accounting for specified boundary conditions leads to:

$$[H_1 \quad H_2 \quad H_3]\begin{pmatrix} u_1 \\ u_2 \\ u_3 \end{pmatrix} = [G_1 \quad G_2 \quad G_3]\begin{pmatrix} t_1 \\ t_2 \\ t_3 \end{pmatrix} + \{f\} \tag{8}$$

$$\{\epsilon\} = -[F_1 \quad F_2 \quad F_3]\begin{pmatrix} u_1 \\ u_2 \\ u_3 \end{pmatrix} + [E_1 \quad E_2 \quad E_3]\begin{pmatrix} t_1 \\ t_2 \\ t_3 \end{pmatrix} + \{g\} \tag{9}$$

The primary unknown in the inverse problem is t_3, and it must be distinguished from other unknowns. Moving $\{t_3\}$ and all known boundary conditions to the right hand side and all other unknowns to the left hand side in Eq.(8) leads to:

$$[-G_1 \quad H_2 \quad H_3]\begin{pmatrix} t_1 \\ u_2 \\ u_3 \end{pmatrix} = [-H_1 \quad G_2 \quad G_3]\begin{pmatrix} u_1 \\ t_2 \\ t_3 \end{pmatrix} + \{f\} \tag{10}$$

rearranging,

$$[A]\{x\} = [G_3]\{t_3\} + \{b_1\} + \{f\} \tag{11}$$

Here $\{x\} = (t_1 \ u_2 \ u_3)^{\mathrm{T}}$ is the secondary unknown vector, $[A]=[-G_1 \quad H_2 \quad H_3]$, and $\{b_1\}$ is a known vector. The secondary unknown vector $\{x\}$ can then be expressed in terms of primary unknown vector $\{t_3\}$ and known quantities as follows:

$$\{x\} = [A]^{-1}[G_3]\{t_3\} + [A]^{-1}\{b_1\} + [A]^{-1}\{f\}) = [G_3']\{t_3\} + \{b_1'\} + \{f'\} \tag{12}$$

The expression of internal strains, Eq. (9), can also be rearranged similarly:

$$\begin{aligned}\{\epsilon\} &= [E_3]\{t_3\} - [\,-E_1 \quad F_2 \quad F_3]\begin{pmatrix} t_1 \\ u_2 \\ u_3 \end{pmatrix} + [\,-F_1 \quad E_2 \quad E_3]\begin{pmatrix} u_1 \\ t_2 \\ 0 \end{pmatrix} + \{g\} \\ &= [E_3]\{t_3\} - [F']\{x\} + \{b_2\} + \{g\}\end{aligned} \tag{13}$$

where $[F'] = [\,-E_1 \ F_2 \ F_3]$, $\{b_2\}$ is a known vector. Substituting Eq.(12) into (13), we arrive at the desired relation in the same form as Eq. (3):

$$\begin{aligned}\{\epsilon\} &= ([E_3] - [F'][G_3'])\{t_3\} + (\{b_2\} - [F']\{b_1'\}) \ + (\{g\} - [F']\{f'\}) \\ &= [C]\{t_3\} + \{b\} + \{d\}\end{aligned} \tag{14}$$

where

$$\begin{aligned}[C] &= [E_3] - [F'][G_3'] \\ \{b\} &= \{b_2\} - [F']\{b_1'\} \\ \{d\} &= \{g\} - [F']\{f'\}\end{aligned} \tag{15}$$

The above relations provide explicit expressions for the matrix $[C]$ and the vectors $\{b\}$ and $\{d\}$ with minimal effort required to implement this formulation in a typical BEM code. The sensitivity matrix $[C]$ and the vectors $\{b\}$ and $\{d\}$ can be formed simultaneously with computational effort comparable to a single BEM forward analysis. This is in sharp contrast to the common practice of calculating $[C]$ by the "unit load" method[3,4] which requires a series of forward problem solutions.

Once matrix $[C]$ and the vectors $\{b\}$ and $\{d\}$ in Eq. (3) are formulated, the primary unknowns $\{t_3\}$ can be solved from measured strains. However, the difficulty is that matrix $[C]$ in Eq. (3) is normally ill-conditioned as a result of

the ill-posedness of the inverse problem. This indicates that a small amount of errors in the measured strains will cause a large amount of error in the computed tractions by directly solving Eq. (3). In previous studies[2,7], global equilibrium conditions were introduced to effectively stabilize the inverse solution process for two-dimensional cases. However, numerical studies showed that the same solution scheme does not provide a stabilized solution for three-dimensional case. In this study, a global approximation of the unknown surface traction for three-dimensional problems is introduced in an effort to reduce the number of the unknowns and to enforce smoothing conditions on the computed tractions. The importance of enforcing smoothing conditions has also been discussed by Tikhonov and Arsinin[11], and Schnur and Zabaras[3].

Surface traction distributions can always be parameterized using only two parameters defining a body-fitted coordinate system. For example, in the case of flat surfaces parallel to a Cartesian coordinate system, a surface traction can be approximated globally as follows:

$$t_3(x,y) = \sum_{i=1}^{L} a_i f_i(x,y) \tag{16}$$

Here, f_i is the basis function, L is the number of basis functions used in the approximation, and a_i are unknown coefficients to be determined. The following polynomial sets are chosen as basis functions (members of the Pascal triangle):

$$\begin{aligned} f_i = \{&1, x, y, x^2, xy, y^2, x^3, x^2y, xy^2, y^3, x^2y^2, \\ &x^4, y^4, x^3y, xy^3, x^5, y^5, x^4y, xy^4, x^3y^2, x^2y^3, \\ &x^3y^3, x^6, y^6, x^5y, xy^5, x^4y^2, x^2y^4, \cdots\} \end{aligned} \tag{17}$$

The unknown parameters are now changed from the traction values at the boundary nodes $\{t_3\}$ to the polynomial coefficients $\{a\}$. The sensitivity matrix must be modified accordingly. The traction values at the boundary nodes can be expressed in terms of the polynomial coefficients as follows:

$$\{t_3\} = [Q]\{a\} \tag{18}$$

Here, $[Q]$ is a transformation matrix and is given as

$$[Q] = \begin{bmatrix} f_1(x_1,y_1) & f_2(x_1,y_1) & \cdots & f_L(x_1,y_1) \\ f_1(x_2,y_2) & f_2(x_2,y_2) & \cdots & f_L(x_2,y_2) \\ \vdots & \vdots & \ddots & \vdots \\ f_1(x_N,y_N) & f_2(x_N,y_N) & \cdots & f_L(x_N,y_N) \end{bmatrix} \tag{19}$$

where x_i and y_i are the coordinates of the i-th boundary node on Γ_3, N is the number of boundary nodes with unknown traction, and L is the number of terms used in the polynomial approximation. Substituting Eq. (18) into Eq. (3) gives the expression for the modified sensitivity matrix:

$$[C_M] = [C][Q] \tag{20}$$

The amount of computation required to obtain the sensitivity matrix for the polynomial traction representation is basically the same as for the piecewise traction representation. It is straightforward to choose the number of terms of the polynomial, in Eq. (17), for some special cases where prior information on the traction distribution is available. Generally, there should be enough terms to closely approximate the unknown function without losing numerical stability. Numerical experiments can usually give some guidance in determining the number of terms to be used in the polynomial.

Unlike a forward problem, in an inverse problem, due to error in measurements, resolved boundary tractions do not strictly satisfy the overall equilibrium conditions. It is thus desirable to explicitly enforce equilibrium conditions as additional constraints. It has been shown that the introduction of these physical constraints has the effect of stabilizing the inverse solution process[5]. To satisfy global equilibrium conditions, the resultant of tractions and moments acting on the boundary must be balanced by body forces. When there is no body force, tractions should be self-balanced. For instance, in the special case of a 3-D problem, in which Γ_3 is parallel to x-y plane, global equilibrium conditions are:

$$\begin{aligned} &\int_{\Gamma_3} t_x \, d\Gamma = \mathrm{I}_1 \ , \ \int_{\Gamma_3} t_y \, d\Gamma = \mathrm{I}_2 \ , \int_{\Gamma_3} t_z \, d\Gamma = \mathrm{I}_3 \\ &\int_{\Gamma_3} (t_y x - t_x y) \, d\Gamma = \mathrm{I}_4 \ , \ \int_{\Gamma_3} t_z y \, d\Gamma = \mathrm{I}_5 \ , \int_{\Gamma_3} t_z x \, d\Gamma = \mathrm{I}_6 \end{aligned} \tag{21}$$

Here, the I_i's are constants and determined from the nature of each individual problem under consideration. The discretized form of global equilibrium constraints can be written in the following matrix form:

$$[D]\{t_3\} = \{\mathrm{I}\} \tag{22}$$

The constraint matrix $[D]$ is determined only by problem geometry and discretization. The same BEM mesh and interpolation model used to obtain the BEM influence matrices $[G]$, $[H]$, $[E]$ and $[F]$ can be used to evaluate the matrix $[D]$. In light of the 3-D global polynomial approximation for $\{t_3\}$ in Eq. (18), matrix $[D]$ should be replaced by $[D_M]$ given as:

$$[D_M] = [D][Q] \tag{23}$$

The constrained least-squares minimization is defined for the inverse problem:

Find : $\{a\}$
to minimize : $([C_M]\{a\} + \{b\} + \{d\} - \{\bar{\epsilon}\})^{\mathrm{T}} \cdot ([C_M]\{a\} + \{b\} + \{d\} - \{\bar{\epsilon}\})$
subject to : $[D_M]\{a\} = \{\mathrm{I}\}$

where vector $\{\bar{\epsilon}\}$ are measured strains. The least squares functional measures the difference between computed and input strains in the L_2 norm, while constraints enforce global equilibrium. Lagrange multipliers are used to adjoin these constraints to the functional. The augmented functional is introduced as

$$F = ([C_M]\{a\} + \{b\} + \{d\} - \{\bar{\epsilon}\})^{\mathrm{T}}([C_M]\{a\} + \{b\} + [d\} - \{\bar{\epsilon}\}) + \{\lambda\}^{\mathrm{T}}([D_M]\{a\} - \{\mathrm{I}\}) \quad (24)$$

Differentiating F with respect to $\{a\}$ and $\{\lambda_i\}$ and setting the result to zero:

$$\begin{bmatrix} [C_M]^{\mathrm{T}}[C_M] & [D_M]^{\mathrm{T}} \\ [D_M] & 0 \end{bmatrix} \begin{Bmatrix} \{a\} \\ \{\lambda\} \end{Bmatrix} = \begin{pmatrix} [C_M]^{\mathrm{T}}(\{\bar{\epsilon}\} - \{b\} - \{d\}) \\ \{\mathrm{I}\} \end{pmatrix} \quad (25)$$

Numerical experimentation reveals that the matrix system of Eq. (25) is well-conditioned. Introduction of the polynomial approximation and physical constraints thus has the desired effect of stabilizing the inverse solution process.

3 Numerical results

In this section, we consider the case of a cube with unknown z-traction on its top surface, see Fig. 1. This cube is constrained at the bottom to prevent rigid body motion. The layout of the sensor locations is shown in Fig. 2, and the BEM mesh is given in Fig. 3. Bilinear isoparametric boundary elements are used. Strain components ϵ_{zz} at 25 measuring points are used as the input to recover the unknown tractions. The following steps are performed in the simulation: (1) the exact traction distribution is assumed, (2) strain values at the measuring locations are computed by a BEM analysis, (3) a level of random error is added to these strain values to simulate input error, and (4) simulated strain measurements are used as the input to the inverse solution. The following conventions are used: (1) referring to strains with $m\%$ error means that a level of $\pm m\%$ random error has been added to the exact strains (2) two numbers in each traction plot stand for the maximum and minimum values of the tractions, (3) a polynomial of n terms means that the first n terms in Eq. (17) are used. In the first example, the exact traction is assumed to be uniform ($t_z(x,y) = 1$). Figure 4 gives the solutions from input strains with 10% random errors. Stable solutions are obtained for all cases, clearly showing that the polynomial representation allows a wide range of error in the input. The overall error of the computed traction is gauged by defining a global error defined as:

$$Rt = \sqrt{\sum_i (\underline{t}_i - t_i)^2} \quad (24)$$

where $\underline{t}_i$ is the computed traction value at sample point "i" and t_i is the exact traction value. Figure 5 shows maximum and global error variation versus error

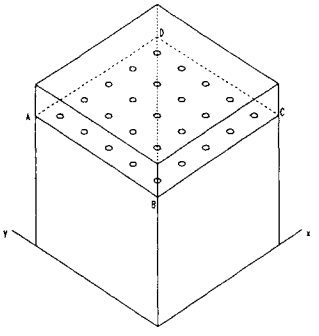

Figure 2. Sensor locations.

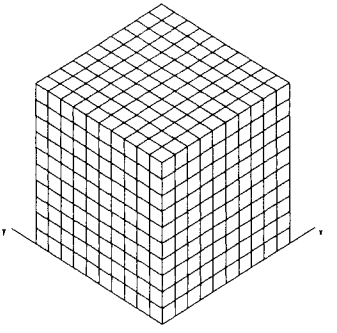

Figure 3. BEM model for a cube.

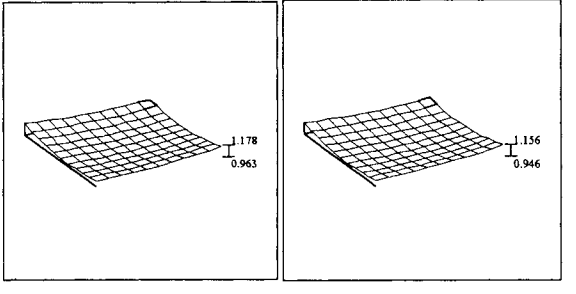

(a) 6 terms, no constraint (b) 6 terms, with constraints

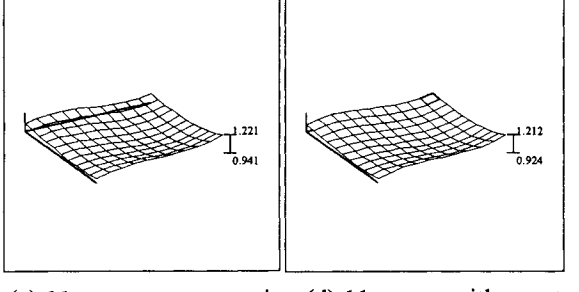

(c) 11 terms, no constraint (d) 11 terms, with constraints

Figure 4. Results of 6 terms and 11 terms with 10% random error in input.

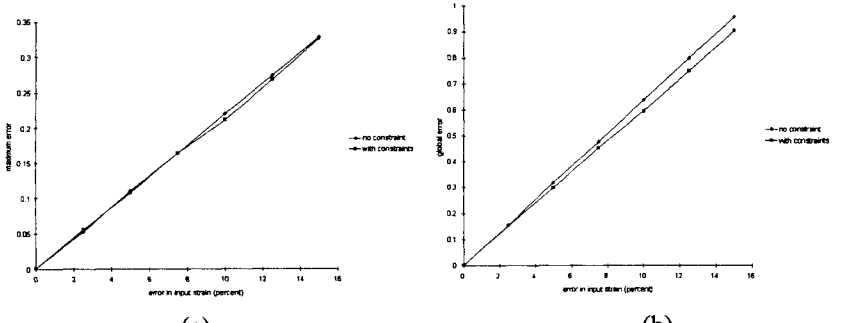

(a) (b)

Figure 5. Error of the computed traction vs. input error (11 terms).

level in input strain. While the difference between the maximum errors with and without constraints is not obvious, the global error with constraints is always lower than the one without constraints. This indicates that constraints effectively improve the computed traction in 3-D problems

The first example represents a special case in which the actual traction distribution is included in the polynomial set. In general, the actual traction distribution can only be approximated by the polynomial. In the second example, the traction is assumed as: $t_z(x,y) = sin(\frac{\pi x}{10})\sin(\frac{\pi y}{10})$. Figure 6 (a)-(d) compares the exact and computed traction using 6, 11 and 15 term polynomials given exact strain input. A six term polynomial is apparently not enough to approximate the actual traction. With 11 or 15 terms, very accurate results are obtained. However, the global error of the 15 term polynomial is smaller than the 11 term polynomial. This is due to the fact that 15 term polynomial is better suited for approximating a higher order unknown function than the 11 term polynomial. The results from input strains with 10% random error are plotted in Fig. 6 (e) and (f), showing that even for 10% error in strain input, the 11 term polynomial gives accurate results. The 15 term solution is more sensitive to input error and its global error is much higher than for the 11 term polynomial.

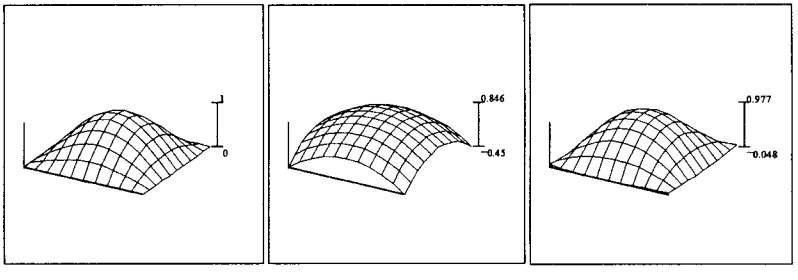

(a) exact distribution (b) 6 terms, Rt=1.449 (c) 11 terms, Rt=0.276

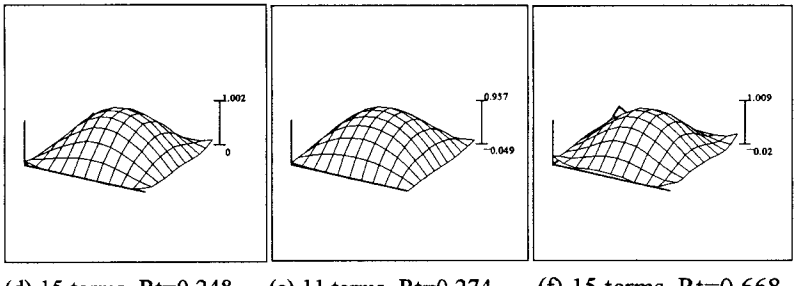

(d) 15 terms, Rt=0.248 (e) 11 terms, Rt=0.274 (f) 15 terms, Rt=0.668

Figure 6. Traction: exact input strains(a)-(d) and 10% input error (e) and (f).

4 Conclusion

A 3-D BEM solution of the inverse traction reconstruction problem is developed. Calculation of the sensitivity matrix is embedded in the BEM, effectively reducing the computational effort involved in its construction. An important step in successfully solving the 3-D inverse problem is the global polynomial approximation for the traction distribution. A constrained least-squares minimization is formulated for the inverse problem. Numerical results demonstrate the method is capable of reconstructing unknown boundary tractions using simulated noisy data.

5 References

1. Sirkis, J.S. and Lo, Y.-L., "Simultaneous measurement of two strain components using 3 $\times$ 3 and 2 $\times$ 2 coupler-based passive demodulation of optical fiber sensors," *IEEE J. Light. Tech.*, Vol.12, 1994, pp.2153-2161.
2. Zhang, F., Kassab, A.J. and Nicholson, D.W., "A boundary element solution of an inverse elasticity problem and applications to determining residual stress and contact stress," *Int. J. Solids and Struct.*(in press).
3. Schnur, D.S. and Zabaras, N., "Finite element solution of two dimensional inverse elastic problems using spatial smoothing," *Int. J. Num. Methds. Eng.*, Vol.30, 1990, pp.57-75.
4. Zhang, F., Kassab, A.J. and Nicholson, D.W., "Application of the boundary element method to measurement of residual stress," *BETECH IX,* C. A. Brebbia and A. J. Kassab (eds.), 1994, pp.165-172.
5. Zhang, F., Kassab, A.J. and Nicholson, D.W., "A boundary element inverse approach for determining residual stress and contact pressure," *Boundary Elements XVII,* Brebbia, C.A., Kim, S., and Osswald, T.,(eds.), 1995, pp.331-338.
6. Yeih, W., Koya, T. and Mura, T., "An inverse problem in elasticity with partially overprescribed boundary conditions, Part 1: Theoretical approach," *J. Appl. Mech.*, Vol.60, 1993, pp.595-600.
7. Zhang, F., "Solution of Two- and Three-Dimensional Inverse Elasticity Problems by BEM and Internal Strain Data," Ph.D. Diss., U. Central Florida, 1996.
8. Martin, T., Halderman, J. and Dulikravich, G., "An inverse method for finding unknown surface traction and deformations in elastostatics," *Comp. Struct.*, Vol.56, 1995, pp.825-835.
9. Bezerra, L. and Saigal, S., "Inverse boundary traction reconstruction with BEM," *Int. J. Solids and Structures,* Vol.32, 1995, pp.1417-1431.
10. Brebbia, C.A., Telles, J.C.F. and Wrobel, L.C., *Boundary Element Techniques*, Springer-Verlag, New York, 1984.
11. Tikhonov, A.N. and Arsenin, V.Y., *Solution of Ill-posed Problems,* John Wiley & Sons, New York, 1977.